Propagation characteristics of the silica and silicon subwavelength-diameter hollow wire waveguides

Man Wu (吴 熳)[1,2], Weiqing Huang (黄维清)[1], and Lingling Wang (王玲玲)[1]

[1]*School of Physics and Microelectronic Science, Hunan University, Changsha 410082*
[2]*Changde Vocational Technical College, Changde 415000*

Received May 20, 2008

The basic propagation properties of the silica and silicon subwavelength-diameter hollow wire waveguides have been investigated by comparison. It shows that the silica and silicon subwavelength-diameter hollow wire waveguides have some interesting properties, such as enhanced evanescent field in the cladding, enhanced intensity in the hollow core, and large waveguide dispersion. For the different confinement ability, the enhanced field in the hollow core and cladding of the silica subwavelength-diameter hollow wire is much stronger than that of the silicon one for the same size.

OCIS codes: 060.2310, 060.2400, 230.7370, 999.9999.
doi: 10.3788/COL20080610.0732.

Dielectric optical waveguides with widths or diameters from micrometers to millimeters have got successful applications in many fields such as optical communication, optical sensing, and optical power delivery systems[1−3]. Many applications benefit from minimizing the width of the waveguides, but fabricating low-loss optical waveguides with subwavelength diameters remains challenging because of high precision requirement. Recently, several types of dielectric sub-micrometer and nanometer diameter wires of optical qualities have been obtained[4−8]. These wires with diameters smaller than 1 μm are tens to thousands times thinner than the commonly used micrometer diameter waveguides. They can be used as air-clad wire-waveguides with subwavelength-diameter cores, and build blocks in the future micro- and nano-photonic devices. These fibers have solid cores and the guiding properties of the waveguides have been adequately studied. However, if the subwavelength-diameter wire is hollow, the guiding characteristics will be different. A team of engineers from the University of California at Riverside has began the exploratory preparation experiments[9] and the subwavelength-diameter hollow wire waveguide offer opportunities for a lot of miniaturized high performance and novel photonic devices[10].

In this paper, based on exact solutions of Maxwell's equations and numerical calculations, the basic guiding properties of silica and the silicon hollow wires have been studied. The refractive index profile is schematically illustrated in Fig. 1. A long straight hollow wire is a cylindrical structure of rotational symmetry involving three regions in the cross section: the hollow core with radius a, dielectric region with radius b, and the infinite air cladding. Refractive indices of the core, dielectric region, and outer cladding are assumed to be n_1, n_2, and n_3, respectively. Translational invariance in the z direction implies that there exists single-spatial-frequency solutions proportional to $\exp(j(wt-\beta z))$, where w is the angular frequency and β is the longitudinal propagation constant[11].

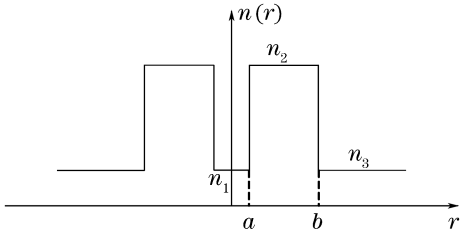

Fig. 1. Cross-section and parameters of the subwavelength-diameter hollow wire waveguide.

The z components of the field, E_z and H_z, satisfy the following Helmholtz equation in the homogeneous sections in which refractive index is constant,

$$[\frac{1}{r}\frac{\partial}{\partial r}(r\frac{\partial}{\partial r})+\frac{1}{r^2}\frac{\partial^2}{\partial\phi^2}+(k_0^2n^2-\beta^2)]\begin{pmatrix}E_z\\H_z\end{pmatrix}=0, \quad (1)$$

where $k_0=wc=w(\mu_0\varepsilon_0)^{1/2}$ is the free-space wave number, ε_0 is the free-space permittivity, and c is the speed of light. For $k_0^2n^2-\beta^2>0$, these equations predict propagating waves with the Bessel functions J_m and Y_m as solutions; and for $k_0^2n^2-\beta^2<0$, they predict exponentially decaying or growing fields with modified Bessel functions I_m and K_m as solutions. Longitudinal field components can be written as

$$E_z=\begin{cases}AI_m(u_1r)f_c, & 0<r<a\\ [BJ_m(u_2r)+CY_m(u_2r)]\,f_c, & a<r<b\\ DK_m(u_3r)f_c, & r>b\end{cases}, \quad (2)$$

$$H_z=\begin{cases}A'I_m(u_1r)f_s, & 0<r<a\\ [B'J_m(u_2r)+C'Y_m(u_2r)]\,f_s, & a<r<b\\ D'K_m(u_3r)f_s, & r>b\end{cases}, \quad (3)$$

where $u_1=\sqrt{\beta^2-k_0^2n_1^2}$, $u_2=\sqrt{k_0^2n_2^2-\beta^2}$, $u_3=\sqrt{\beta^2-k_0^2n_3^2}$, $f_c=\cos(m\phi+\varphi_m)\exp[j(wt-\beta z)]$, and $f_s=\sin(m\phi+\varphi_m)\exp[j(wt-\beta z)]$.

The transverse field components are obtained from the

following equations:

$$E_r = -\frac{j}{k_0^2 n^2 - \beta^2}\left(\beta\frac{\partial E_z}{\partial r} + \frac{w\mu_0}{r}\frac{\partial H_z}{\partial \phi}\right), \tag{4a}$$

$$E_\phi = -\frac{j}{k_0^2 n^2 - \beta^2}\left(\frac{\beta}{r}\frac{\partial E_z}{\partial \phi} - w\mu_0\frac{\partial H_z}{\partial r}\right), \tag{4b}$$

$$H_r = -\frac{j}{k_0^2 n^2 - \beta^2}\left(\beta\frac{\partial H_z}{\partial r} - \frac{w\varepsilon_0 n^2}{r}\frac{\partial E_z}{\partial \phi}\right), \tag{4c}$$

$$H_\phi = -\frac{j}{k_0^2 n^2 - \beta^2}\left(\frac{\beta}{r}\frac{\partial H_z}{\partial \phi} + w\varepsilon_0 n^2\frac{\partial E_z}{\partial r}\right). \tag{4d}$$

Applying boundary conditions at $r = a$ and $r = b$, a system of eight linear homogeneous equations is obtained that is satisfied by the eight coefficients. The propagation constant β is determined by the condition that the determinant of the system of linear equations should vanish[12]:

$$\det[M(\beta)] = 0, \tag{5}$$

where M is the resulting matrix of the system of equations. The power flow (power density) along the z direction in cylindrical coordinates is given by[11]

$$S_z = \frac{1}{2}\Re[E_r H_\phi^* - E_\phi H_r^*]. \tag{6}$$

We assume that the index of the air (n_1 and n_3) is 1.0, and use the following Sellmeier-type dispersion formula (at room temperature) to obtain the refractive indices of the wire materials for fused silica[13]:

$$n^2 - 1 = \frac{0.6961663\lambda^2}{\lambda^2 - (0.0684043)^2} + \frac{0.4079426\lambda^2}{\lambda^2 - (0.1162414)^2} + \frac{0.8974794\lambda^2}{\lambda^2 - (9089616)^2}, \tag{7}$$

for single crystal silicon:

$$n^2 = 11.6858 + \frac{0.939816}{\lambda^2} + \frac{0.000993358}{\lambda^2 - 1.22567}, \tag{8}$$

where the unit of λ is μm.

For the convenience, we use normalized propagation constant B to characterize the wire and it is defined by $B = (\beta^2 - k_0^2 n_3^2)/(k_0^2 n_2^2 - k_0^2 n_3^2)$. Figure 2 shows the variation of B with respects to wavelength for HE_{11}, TE_{01}, and TM_{01} modes in the silica and silicon hollow wires with parameters: $a = 10$ nm, $b = 100$ nm. With the increase of wavelength, B parameter decreases and becomes zero when λ approaches about 1 μm for HE_{11} mode. For TE_{01} and TM_{01} modes, they become cutoff at a relatively shorter wavelength. For the same mode, the silicon hollow wires have higher B parameter and longer cutoff wavelength than the corresponding silica hollow wires.

If b is set to be constant 100 nm and a varies, the B parameter increases with the decrease of a/b and wavelength, as shown in Fig. 3. It also can be seen that B increases with the narrower hollow core. With the increase of B parameter, the hollow wire will confine light energy much easier.

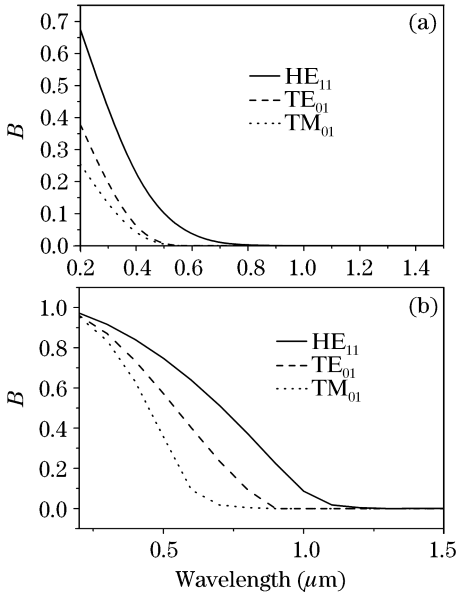

Fig. 2. Variation of B with wavelength for the three lowest order modes for (a) the silica hollow wire and (b) the silicon hollow wire.

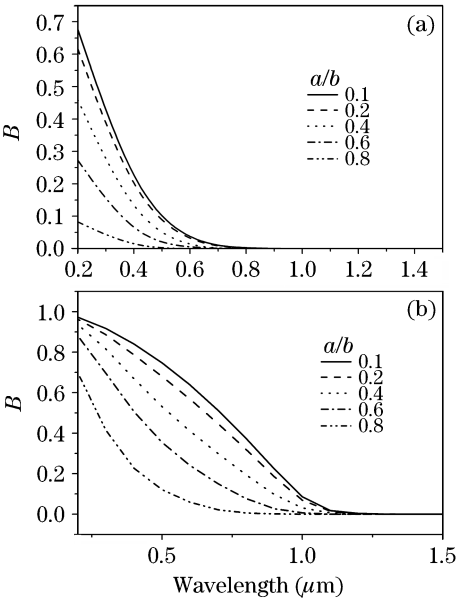

Fig. 3. Variation of B with wavelength for the hollow wire with a/b for (a) the silica hollow wire and (b) the silicon hollow wire.

In practical applications, such as evanescent wave based optical devices, it is important to know the profile of the power distribution around the waveguide. Here, the wires are all operated in single mode. Profiles of power density for the silica hollow wires at 633 nm wavelength are shown in Fig. 4(a), in which the mesh profile stands for the propagation field inside the dielectric region, and the gradient profile stands for the evanescent fields in air. To clarify the influence of the central hole on the properties of the hollow wire, the power density of the subwavelength-diameter wire without central hole (core size 100 nm) has been plotted in Fig. 4(b). As can be seen, the hollow wire leaves a large amount of light guided outside as evanescent waves[14]. The intensity in

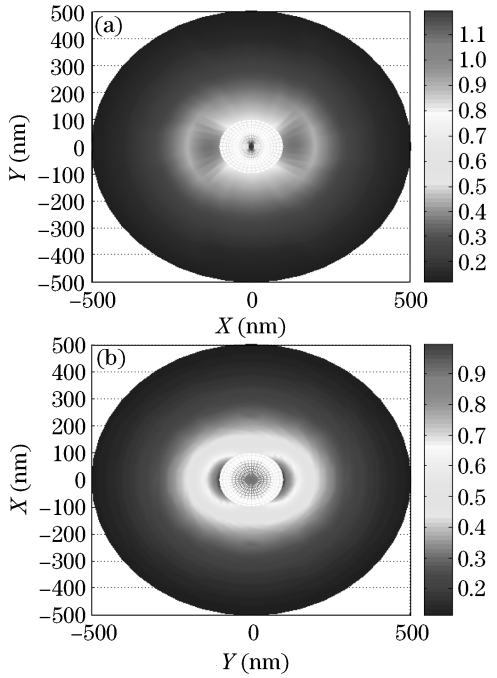

Fig. 4. z-direction power density of (a) the silica hollow wire with $a/b = 0.1$ and $b = 100$ nm, (b) the subwavelength-diameter silica wire with core size 100 nm. Mesh, field inside the dielectric region. Gradient, field outside the dielectric region.

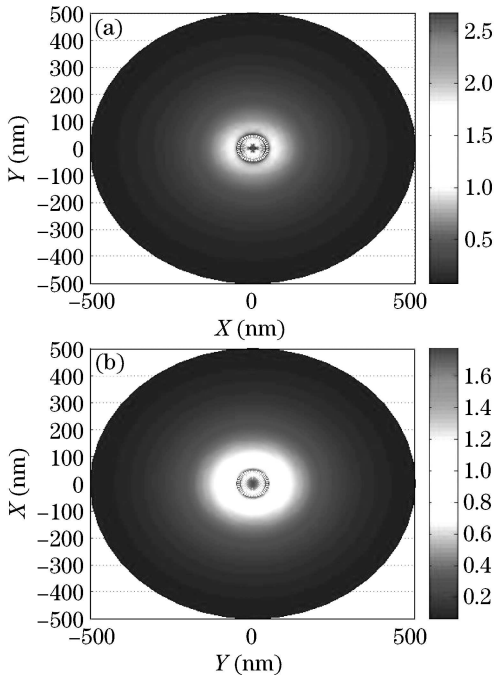

Fig. 5. z-direction power density of (a) the silicon hollow wire with $a/b = 0.2$ and $b = 50$ nm, (b) the subwavelength-diameter silicon wire with core size 50 nm. Mesh, field inside the dielectric region. Gradient, field outside the dielectric region.

central hollow region of the hollow wire has been enhanced, and the region is filled with air. The enhanced intensity results from the discontinuity of the electric field at the interface between the hollow region and the dielectric region[15,16]. For the small size of this central air hole, the decay of the evanescent wave within the hole is minimal, and the enhanced field intensities are achieved throughout the hole. Furthermore, the power density of the silicon hollow wire and the corresponding subwavelength-diameter solid core wire are shown in Fig. 5. The silicon dielectric region can confine the light energy well, so the evanescent wave outside the core region is relatively weak compared with the silica wire in Fig. 4. For the central hollow region, the silicon hollow wire also has enhanced intensity compared with the corresponding solid core subwavelength-diameter wire. The enhanced intensity in the central region may open up the prospect of using these holes as sites for interacting intense light with materials located within the air void. For the cases discussed based on the vectorial model, the power distributions are not symmetric rotationally and have strong dependence on the azimuthal angle[11,14].

To clarify the magnitude of enhancement, we define the maximum enhancement factor as the ratio of the maximum power density in the central region of the hollow wire and that of the corresponding subwavelength-diameter wire without the central hollow region. In the calculation, we set the power densities of the hollow wire and the subwavelength-diameter wire equal at the interface of dielectric region and the outermost air cladding. If $a = 10$ nm and $b = 100$ nm, it can be obtained that the maximum enhancement factor is 1.33 for the silica hollow wire.

With propagation constants obtained by numerically solving Eq. (5), the group velocities v_g and waveguide dispersions D_w can be obtained[13]. The wavelength-dependent waveguide dispersions of the silica and silicon hollow wire are shown in Fig. 6. It can be seen clearly that the waveguide dispersions of these wires can be very large compared with those of weakly guiding fibers. Results also show that, large dispersion shift can be obtained by changing the central hollow region. Controlling light propagation properties by tailoring waveguide

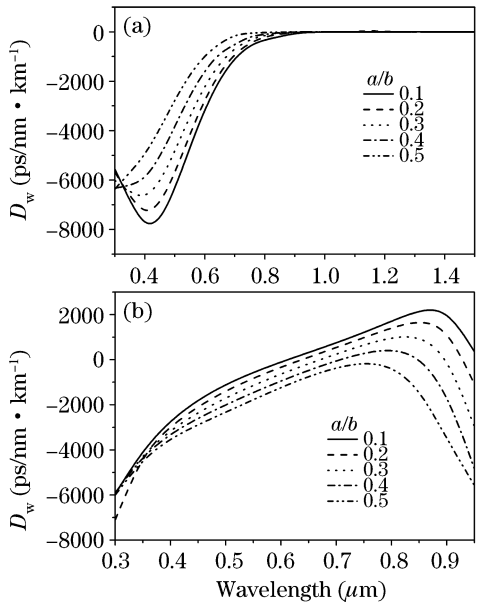

Fig. 6. Wavelength-dependent waveguide dispersion of fundamental modes of (a) the silica hollow wire and (b) the silicon hollow wire with different a/b.

dispersion are used in many fields such as optical communication and nonlinear optics, therefore, these wires present opportunities for achieving enhanced dispersions with reduced sizes.

Here, the polarization dependence of the structure has been studied. By using Eqs. (2)—(4), we can get $E_r/|E_r| = E_\varphi/|E_\varphi|$, so E_r and E_φ have the same phase. Therefore, the vector orientation of the total transverse component does not vary in time. Thus the transverse component of the field is linearly polarized with respect to the time evolution at each fixed spatial point (r, ϕ). Meanwhile, the phase of the longitudinal component E_z differs from that of the transverse components E_r and E_φ by $\pi/2$. Due to this phase difference, the total electric field rotates elliptically with time. Thus the properties of the exact fundamental mode HE_{11} may become substantially different from the linearly polarized mode LP_{01}.

In conclusion, we have studied the basic properties of the subwavelength-diameter silica and silicon hollow wires. We assume the wires are ideally uniform in terms of the sidewall smoothness and diameter uniformity. Compared with large core optical waveguides, the hollow wires show some interesting properties, such as enhanced evanescent field, enhanced intensity in the hollow region, and large waveguide dispersion, which may offer opportunities for developing a number of miniaturized high performance and novel photonic devices.

M. Wu's e-mail address is manmwu@gmail.com.

References

1. B. E. A. Saleh and M. C. Teich, *Fundamentals of Photonics* (John Wiley and Sons, New York, 1991).
2. J. Fu, X. Yin, N. Li, and L. Tong, Chin. Opt. Lett. **6,** 112 (2008).
3. Z. Zhang, M. Qiu, U. Andersson, and L. Tong, Chin. Opt. Lett. **5,** 577 (2007).
4. L. M. Tong, R. R. Gattass, J. B. Ashcom, S. L. He, J. Y. Lou, M. Y. Shen, I. Maxwell, and E. Mazur, Nature **426,** 816 (2003).
5. G. Brambilla, V. Finazzi, and D. J. Richardson, Opt. Express **12,** 2258 (2004).
6. S. Leon-Saval, T. A. Birks, W. J. Wadsworth, P. St. J. Russell, and M. Mason, Opt. Express **12,** 2864 (2004).
7. M. Sumetsky, Y. Dulashko, and A. Hale, Opt. Express **12,** 3521 (2004).
8. M. Sumetsky, Y. Dulashko, J. M. Fini, and A. Hale, Appl. Phys. Lett. **86,** 161108 (2005).
9. L. M. Huang, H. T. Wang, C. Y. Hayashi, B. Z. Tian, D. Y. Zhao, and Y. S. Yan, J. Mater. Chem. **13,** 666 (2003).
10. C. Zhao, Z. Tang, Y. Ye, D. Fan, L. Qian, S. Wen, and G. Chen, Opt. Express **15,** 6629 (2007).
11. E. Karadeniz and P. Kornreich, Opt. Eng. **45,** 085001 (2006).
12. J. Y. Lou, L. M. Tong, and Z. Z. Ye, Opt. Express **14,** 6993 (2006).
13. G. Agrawal, *Nonlinear Fibre Optics* 2nd edn. (Academic, New York, 1994).
14. L. M. Tong, J. Y. Lou, and E. Mazur, Opt. Express **12,** 1025 (2004).
15. V. R. Almeida, Q. Xu, C. A. Barrios, and M. Lipson, Opt. Lett. **29,** 1209 (2004).
16. G. S. Wiederhecker, C. M. B. Cordeiro, F. Couny, F. Benabid, S. A. Maier, J. C. Knight, C. H. B. Cruz, and H. L. Fragnito, Nature Photon. **1,** 115 (2007).